Internal conversion between bound states and the Pauli exclusion principle

F. F. Karpeshin,[1,2,3] M. B. Trzhaskovskaya,[4] M. R. Harston,[1,5] and J. F. Chemin[1]
[1]*Centre d'Etudes Nucléaires de Bordeaux-Gradignan, 33175 Gradignan, France*
[2]*Universidade de Coimbra, Departamento de Física, P-3004-516 Coimbra, Portugal*
[3]*Institute of Physics, St. Petersburg University, 198904 St. Petersburg, Russia*
[4]*Petersburg Nuclear Physics Institute, 188350 Gatchina, Russia*
[5]*Service de Physique Nucléaire, CEA/DAPNIA, Orme des Merisiers, 91191 Gif sur Yvette, France*
(Received 7 March 2001; published 6 February 2002)

We present the results of an investigation of the contribution to decay of the nucleus by an unexplored mode of internal conversion in which an excited nuclear state deexcites with promotion of an electron to an intermediate filled bound state. This process, which apparently violates the Pauli exclusion principle, may make a significant contribution to the nuclear decay rate when very close matching of the atomic and nuclear transitions is achieved. For an $M1$ transition, we show that Pauli-forbidden bound internal conversion (PFBIC) transition may occur by excitation of an inner electron to an initially occupied outer orbital. Numerical calculations of the PFBIC process are presented for the decay of the 77.351 keV level of ^{197}Au, in the neutral atom and in ions up to 69^+. The PFBIC process is found to have a maximum probability in ^{197}Au ions with charge state of approximately 40^+, due to close energy matching of the nuclear transition to the $1s \rightarrow 3s$ electronic excitation. The expected dependence of the nuclear lifetime on PFBIC is analyzed.

DOI: 10.1103/PhysRevC.65.034303 PACS number(s): 23.20.Nx, 23.20.Lv

I. INTRODUCTION

One of the consequences of the relativistic quantum theory of electromagnetic interactions is the fact that transitions can take place to intermediate states that are forbidden by the Pauli exclusion principle [1,2]. Examples of processes for which the transition rate contains contributions from states that apparently violate the Pauli principle include radiative electron capture [2,3], radiative β decay [4], Compton excitation of nuclear levels [5,6], the exchange correction in electron capture decay [7–9], the exchange effect in β^- decay [10], and two photon decay of atomic inner shells [11–14]. The exchange effects in electron capture decay [9] and β^- decay [15] have been confirmed experimentally.

In this paper we discuss the case of apparent violation of the Pauli principle in nuclear electromagnetic decay processes, specifically the process called BIC (bound internal conversion) [16–18] in which a nucleus, initially in an excited state, undergoes a transition to a lower-lying state with excitation of an electron to a previously empty bound final state orbital located below the ionization threshold. Evidence for this process, which has sometimes been referred to as TEEN or subthreshold internal conversion, has recently been presented in highly charged *Te* ions [18]. BIC is the inverse of the NEET process [19–21] (nuclear excitation by electron transition) in which a nucleus is excited by a near-resonant transition of an initially excited electron state. The observation of such a resonant energy transfer between the electronic part of the atom and the nucleus has been recently reported in ^{197}Au [22,23]. Hereafter we consider the case of BIC nuclear deexcitation, when the intermediate state bound orbital is fully occupied. This process, which apparently violates the Pauli principle, is hereafter referred to as Pauli-forbiden bound internal conversion (PFBIC).

We take the $M1$ decay of the 77.351 ∓ 0.002 keV excited level of ^{197}Au as an example of the PFBIC process. The main channels for the decay of this excited state proceed by emission of an $M1$ γ or by normal internal conversion (IC) to final electronic states in the continuum. IC occurs principally in the $2s$ and $3s$ shells and corresponds to a total internal conversion coefficient of approximately 4.2. The half-life of the first excited state is 1.91 ∓ 0.01 ns [24]. Our aim here is to investigate the contribution of PFBIC to the nuclear decay rate and its dependence on the ionization state. In PFBIC in ^{197}Au, a virtual photon from the nucleus interacts with a $1s$ electron creating a hole in the K shell. The lifetime of the K-shell vacancy is very short due to the strength of the radiative dipole transition $2p \rightarrow 1s$. This lifetime corresponds to a hole width of the order of 52 eV that facilitates energy matching between the nuclear transition energy and the atomic $1s \rightarrow 3s$ electronic excitation energy (77 300 eV). An essential feature of PFBIC is the formation of a virtual $3s$ hole that can be occupied by the electron excited from the 1s shell. Several mechanisms can contribute to the formation of such a virtual hole. One possibility is the double transition $2p \rightarrow 1s$ and $3s \rightarrow 2p$ with emission of two photons in the final state. A related possibility is the transition $2p \rightarrow 1s$ together with filling of the $2p$ hole by an Auger transition leading to the excitation of a $3s$ electron and emission of an Auger electron into the continuum. A third possibility is filling of the initial $1s$ hole by an Auger transition that excites a $3s$ electron into the continuum. In the final state for PFBIC the virtual $3s$ hole has been filled so that the Pauli principle is indeed satisfied in this state. The creation and filling of this intermediate virtual hole necessarily imply that PFBIC involves terms of higher order in the perturbation series than the usual internal conversion process. This is the price to be paid for temporarily violating the Pauli principle.

We choose the nucleus ^{197}Au for a first investigation of PFBIC effects because the excitation energy from the $1s$ shell to the $3s$ shell lies within 100 eV of the nuclear excitation energy in the neutral atom so that the Pauli-forbidden transition $1s \rightarrow 3s$ is nearly resonant with the nuclear transi-

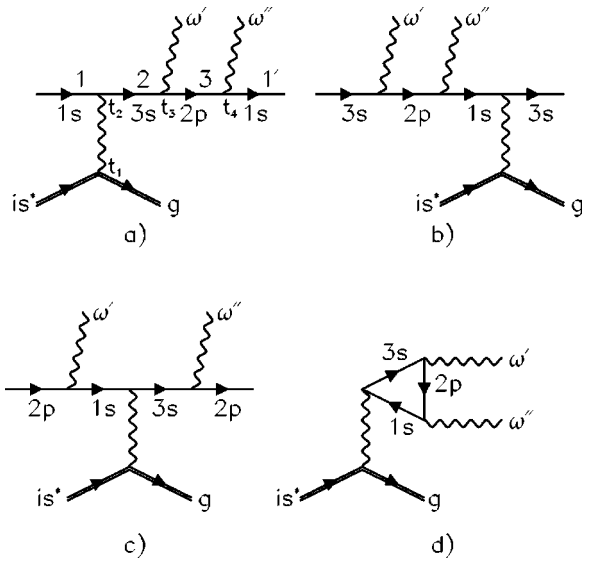

FIG. 1. Feynman diagrams representing the PFBIC process in an $M1$ transition from an isomeric nuclear state (denoted is) to the ground nuclear state (denoted g) with electron excitation from the $1s$ shell to the $3s$ shell.

tion. In addition, we examine the charge state dependence of the PFBIC rate since the atomic binding energies change with the charge state, thereby allowing the possibility that the PFBIC transition lies closer to resonance in ionized states [25]. For reasons of simplicity, we start with a formal description of the PFBIC in the case of two photon emission. The rates for PFBIC decays associated with Auger processes are subsequently derived.

II. PAULI-FORBIDDEN BIC DECAY IN AN $M1$ TRANSITION

Feynman diagrams for the PFBIC process are shown in Fig. 1. We start from an initial state in which the neutral atom of ^{197}Au contains the nucleus in the first excited state. A γ quantum, emitted by the nucleus, scatters on the K-shell electrons, one of them being virtually excited by the $M1$ transition into the $3s$ state. An interpretation of Fig. 1(a) is displayed in Fig. 2. At the instant of time, $t_4 > t_3$, spontaneous vacuum production of the electron-positron pair e^+e^- occurs, with emission of a photon of energy ω''. The electron thus created occupies the $1s$ state. The positron moving backwards in time annihilates with the $2p$ electron "2" at the instant $t_2 < t_3$, and, in doing so, a vacancy for the transition $3s \rightarrow 2p$ is prepared. In a similar manner, at the instant of time t_3 a second e^+e^- pair is produced and the photon ω' is emitted. The electron is created in the $2p$ state. The positron moves backwards in time and annihilates with the $3s$ electron at the time $t_2 < t_3$, thereby preparing the vacancy for the conversion transition $1s \rightarrow 3s$. The contribution of the unconnected diagram in Fig. 2 is exactly equal to the amplitude of the process shown in Fig. 1(a). It is for this reason that, in general, disconnected diagrams are not considered explicitly. Instead one considers diagrams of the type presented in Fig. 1(a), irrespective of the fact that the Pauli principle is apparently violated [1]. Here, the initial and final electron states are denoted "1" and "1′," whilst the intermediate electronic states are denoted "2" and "3." The sequence of interactions in time $t_1 < t_2 < t_3 < t_4$ is indicated. Additional Feynman diagrams relating to the same process are given in Figs. 1(b) and 1(c). These are equivalent to the diagram of Fig. 1(d). Let us consider the latter graph.

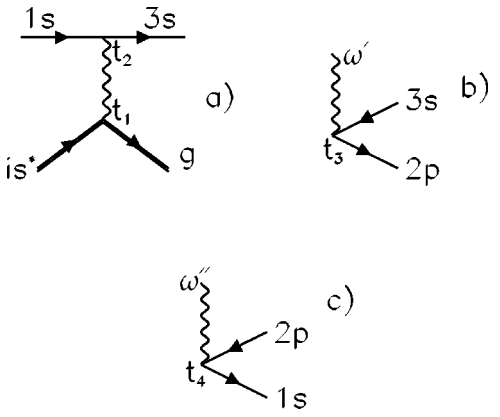

FIG. 2. Unconnected Feynman diagrams associated with the PFBIC process for the same transition as shown in Fig. 1. Their contribution is exactly equal to that of the diagram in Fig. 1(a).

In the fourth order of the perturbation theory we can write expression for the S matrix [26] as

$$S = Te^{-ie\int L d^4x} \simeq (-ie)^4 \int d^4x_1 \ldots d^4x_4 T\{J_\mu(x_4)\mathcal{D}^{\mu\nu}(x_4 - x_1) : \bar{\psi}(x_1)\gamma_\nu \psi(x_1) : \mathcal{A}^\lambda(x_2) : \bar{\psi}(x_2)\gamma_\lambda \psi(x_2) : \mathcal{A}^\rho(x_3) : \bar{\psi}(x_3)\gamma_\rho \psi(x_3)\} :, \tag{1}$$

where ψ and $\bar{\psi}$ are the Dirac field operators

$$\psi(x) = \sum_{\omega>0} a_\omega \psi_\omega(\vec{r}) e^{-i\omega t} + \sum_{\omega<0} b_\omega^+ \psi_\omega(\vec{r}) e^{i\omega t}. \tag{2}$$

The quantities $\mathcal{A}^\lambda(x)$ are the operator electromagnetic potentials. $J_\mu(x_4)$ is the four vector of the nuclear current. $\mathcal{D}^{\mu\nu}$ is a photon propagator. The normal product in Eq. (1) is indicated by colons. We recall that the form of normal

products means that annihilation operators are put to the right of creation operators when they are in the same product. In Eq. (1) the symbol $\underbrace{\quad}$ shows possible ways of contraction that enables us to mutually cancel spectator creation and annihilation operators, expressing them in terms of electron propagators [26]

$$\langle 0|T\{\psi(x)\underbrace{\bar{\psi}(y)}\}|0\rangle = G(x-y). \tag{3}$$

The amplitude of the process is

$$\langle \Psi_2|S^{(4)}|\Psi_1\rangle, \tag{4}$$

where Ψ_1 is the wave function of the initial electronic state with q electrons

$$\Psi_1 = \prod_{i=1}^{q} a_i^+|0\rangle, \tag{5}$$

and the state $|0\rangle$ is the vacuum state. For the first case mentioned above of PFBIC with two photon emission, the wave function Ψ_2 describes the state of the q electrons and two photons with energies ω_1 and ω_2 in the final state and can be written

$$\Psi_2 = \frac{c^+_{\omega_1} c^+_{\omega_2}}{\sqrt{4\omega_1\omega_2}}\Psi_1, \tag{6}$$

where $c^+_{\omega_{1,2}}$ are the associated photon creation operators. After substitution of expressions (1) and (2) into Eq. (4) all the creation and annihilation operators can be transposed to the left of the operators a^+ and a entering the definitions of the wave functions Eqs. (5) and (6). This enables the fermion operators to cancel with one another.

We now employ the spectral representation of the Green's function for electrons having an energy E in the intermediate states [see Fig. 1(d)]

$$G_E(\mathbf{r},\mathbf{r}') = \sum_n \frac{\psi_n\rangle\langle\overline{\psi}_n}{E-\epsilon_n+i\dfrac{\Gamma_n}{2}}, \tag{7}$$

where the wave functions ψ_n form a complete set of one-electron eigenfunctions of the Dirac equation in the self-consistent potential of an average field. The imaginary part in the denominator of Eq. (7) is equal to half the total width of the electron state n. We restrict ourselves to one term in the expansion of Eq. (7), involving the eigenenergy that is, closest to the resonance, that is, the term corresponding to the $3s$ state in the Au atom. This assumption is justified by experimental spectra of photons emitted in the two photon deexcitation of $M1$ transitions in heavy atoms. They show pronounced maxima in the photon energy distribution at energies of discrete $E1$ transitions $3s\rightarrow 2p$ ans $1s\rightarrow 2p$ [12,14]. We obtain the following approximate expression for the Green's function:

$$G_E^{(3s)}(\mathbf{r},\mathbf{r}') \simeq \frac{\psi_{3s}\rangle\langle\overline{\psi}_{3s}}{E-\epsilon_{3s}+i\dfrac{\Gamma_{3s\rightarrow 2p}}{2}}. \tag{8}$$

Analogously, for the $2p$ shell electron we obtain

$$G_E^{(2p)}(\mathbf{r},\mathbf{r}') \simeq \frac{\psi_{2p}\rangle\langle\overline{\psi}_{2p}}{E-\epsilon_{2p}+i\dfrac{\Gamma_{2p\rightarrow 1s}}{2}}, \tag{9}$$

and for the $1s$ electron

$$G_E^{(1s)}(\mathbf{r},\mathbf{r}') \simeq \frac{\psi_{1s}\rangle\langle\overline{\psi}_{1s}}{E-\epsilon_{1s}+i\dfrac{\Gamma_h}{2}}. \tag{10}$$

Here $\Gamma_{3s\rightarrow 2p}$ and $\Gamma_{2p\rightarrow 1s}$ are the total widths of the corresponding transition, and Γ_h is the 1s hole width. Using Eqs. (4), and Eqs. (8)–(10) yields the following expression for the amplitude of the process with emission of two photons in the final state shown in Fig. 1(a):

$$F^{\gamma_1\gamma_2}_{PFBIC} = \sum_j \int F_c \frac{F_\gamma(\omega';3s\rightarrow 2p_j)}{\left(-\omega+i\dfrac{\Gamma_h}{2}\right)\left(\omega_n+\omega-\epsilon_{3s}+i\dfrac{\Gamma_{3s\rightarrow 2p}}{2}\right)} \times \frac{F_\gamma(\omega'';2p_j\rightarrow 1s)}{\left(\omega_n+\omega-\omega'-\epsilon_{2p}+i\dfrac{\Gamma_{2p\rightarrow 1s}}{2}\right)}\frac{d\omega}{2\pi i}. \tag{11}$$

In this equation, F_c is the amplitude for the conversion of the nucleus with electron promotion $1s\rightarrow 3s$, $F_\gamma(\omega';3s\rightarrow 2p_j)$ is the amplitude of the radiative transition $3s\rightarrow 2p_j$ and $F_\gamma(\omega'';2p_j\rightarrow 1s)$ the amplitude of the radiative transition $2p_j\rightarrow 1s$, with j the total angular momentum of the p orbital, equal to 3/2 or 1/2.

Closing the contour in the upper half plane of ω, where the integrand in Eq. (11) has one pole at $\omega = i(\Gamma_h/2)$, we find

$$F^{\gamma_1\gamma_2}_{PFBIC} = \frac{\sum_j F_c F_\gamma(\omega';3s\rightarrow 2p_j)F_\gamma(\omega'';2p_j\rightarrow 1s)}{\left(\Delta+i\dfrac{\Gamma_{3s\rightarrow 2p}+\Gamma_h}{2}\right)\left(\omega_n-\omega'-\epsilon_{2p}+i\dfrac{\Gamma_{2p\rightarrow 1s}+\Gamma_h}{2}\right)}. \tag{12}$$

In Eq. (12), $\Delta = \epsilon_{3s}-\epsilon_{1s}-\omega_n$ is the energy difference between the electronic transition $1s\rightarrow 3s$ and the energy of the nuclear transition. The photon energies are related to the nuclear transition energy by energy conservation, so that $\omega'+\omega''=\omega_n$. Details of the calculation for the partial width of the PFBIC process are given in Appendix A. We obtain

$$\Gamma^{\gamma_1\gamma_2}_{PFBIC}=\sum_j S_j \frac{\alpha_d\Gamma^{(n)}_\gamma}{\Delta^2+\left(\frac{\Gamma_{3s\to 2p}+\Gamma_h}{2}\right)^2}\frac{\Gamma^{3s\to 2p_j}_\gamma\Gamma^{2p_j\to 1s}_\gamma}{2\pi\Gamma^{(t)}_h}, \tag{13}$$

where j is the spin of the intermediate state, S_j is a statistical factor, $\Gamma^{(n)}_\gamma$ is the nuclear radiative width, $\Gamma^{3s\to 2p_j}_\gamma$ is the radiative width of the $3s\to 2p_j$ electron trasition, $\Gamma^{2p_j\to 1s}_\gamma$ is the radiative width of the $2p_j\to 1s$ transition, $\Gamma^{(t)}_h=\Gamma_h+\Gamma^{2p_j\to 1s}_\gamma$ is the combined width of the $1s$ hole and the width of the $2p_j\to 1s$ radiative transition, and α_d is the discrete internal conversion coefficient [27]. Dividing Eq. (13) by the radiative nuclear width, we obtain an expression for the ratio, R_{PFBIC}, of the rate for PFBIC decay in the two photon channel to the rate for nuclear radiative decay,

$$R^{\gamma_1\gamma_2}_{PFBIC}=\sum_j S_j \frac{\alpha_d}{\Delta^2+\left(\frac{\Gamma_{3s\to 2p}+\Gamma_h}{2}\right)^2}\frac{\Gamma^{3s\to 2p_j}_\gamma\Gamma^{2p_j\to 1s}_\gamma}{2\pi\Gamma^{(t)}_h}. \tag{14}$$

The coefficient R_{PFBIC} is analogous to the internal conversion coefficient for decay of an excited nuclear level. The rate for PFBIC is seen to be proportional to the product of the widths for each Pauli-forbidden intermediate state. In the limit that the widths tend to zero, the PFBIC process becomes strictly forbidden.

We can compare the result of Eq. (14) with the result in Ref. [27] for BIC decay to a final state orbital that is unoccupied in the initial state. In this case there is no violation of the Pauli principle and only the $1s$ hole width appears in the BIC decay rate. In this situation the ratio of BIC decay to nuclear radiative decay is given by:

$$R_{BIC}=\frac{\alpha_d\Gamma_h}{2\pi[\Delta^2+(\Gamma_h/2)^2]}. \tag{15}$$

The internal conversion coefficient for PFBIC as given by Eq. (14) corresponds to the case where two photons are present in the final state. In fact the transition $3s\to 2p$ does not need to be a radiative one. Any transition leading to a virtual hole in the $3s$ shell and enabling the promoted $1s$ electron to fill this hole can contribute to the width for PFBIC. This is the case for an Auger transition of the type LM_1Y where L, M_1, and Y, respectively, stand for an initial $2p$ vacancy, and final state holes in the $3s$ and in an outer shell Y. In the calculation of the contribution to PFBIC for this process, corresponding to one photon and one electron in the continuum, the partial width $\Gamma^{3s\to 2p_j}_\gamma$ in Eq. (14) should be replaced by a partial Auger-width $\Gamma^{3s\to 2p_j}_{LM_1Y}$. Assuming identical statistical S_j factors enter in the expressions of the radiative and Auger PFBIC, the partial nonradiative internal coefficient $R^{\gamma_1,LM_1}_{PFBIC}$ can be written

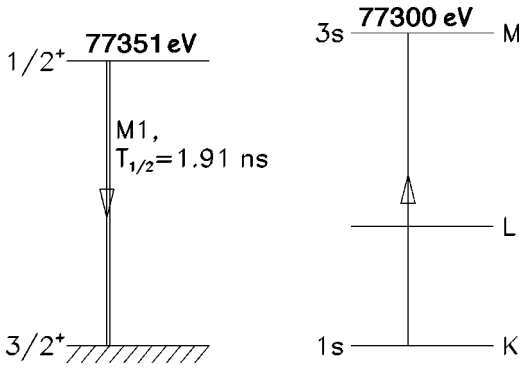

FIG. 3. Nuclear and electronic levels of ^{197}Au in the neutral atom. The nuclear levels are shown on the left and the electronic levels on the right-hand side.

$$R^{\gamma_1,LM_1}_{PFBIC}=\frac{R^{\gamma_1\gamma_2}_{PFBIC}}{w_{2p}}, \tag{16}$$

where w_{2p} is the Auger yield of a $2p$ hole.

There is an additional channel for PFBIC where the virtual state goes over to a final state in a one step process. This can occur in the case of the decay of the $1s$ hole state by a K-shell Auger process directly producing a hole in the M_1 shell, which can be filled by the converted electron. The Auger transitions KL_1M_1, $KL_{23}M_1$, KM_1M_1, and so forth, denoted below by KXM_1, lead to a final state after conversion with only one electron in the continuum. An electron defined by the angular momentum quantum numbers j_3 and m_3, with binding energy ϵ_3, fills the K-shell vacancy, knocking the $3s$ electron into a continuum state defined by the quantum numbers j_p and m_p. The energy of the continuum electron is thus given in terms of the binding energy of the electron in the shell X by

$$\epsilon_e=\omega_n-\epsilon_X. \tag{17}$$

Analogously to the process of Fig. 1(d), the amplitude for the diagram in Fig. 3 can be written

$$F^{KXM_1}_{PFBIC}=\sum_{m_1,m_2,m}\int\frac{F_cF_{KXM_1}}{\left(-\omega+i\frac{\Gamma_h}{2}\right)\left(\omega_n-\omega-\epsilon_{3s}+i\frac{\Gamma_{3s}}{2}\right)}\frac{d\omega}{2i\pi}, \tag{18}$$

where F_{KXM_1} is the amplitude for the Auger process, Γ_{3s} is the partial width for the creation of a hole in the $3s$ orbital in a K-Auger process and m_1, m_2, and m are the magnetic quantum numbers of the $1s$ electron $3s$ electron and virtual photon, respectively. Carrying out the integration over the energy ω in Eq. (18) yields

$$F^{KXM_1}_{PFBIC}=\sum_{m_1,m_2,m}\frac{F_cF_{KXM_1}}{\left(\omega_n-\epsilon_{3s}+i\frac{\Gamma_h+\Gamma_{3s}}{2}\right)}. \tag{19}$$

TABLE I. The radiative widths Γ_{nl} (in eV) of the $nl \rightarrow 1s$ transitions contributing to the total width of the hole $1s$ state in ^{197}Au.

nl	$2p_{1/2}$	$2p_{3/2}$	$3p_{1/2}$	$3p_{3/2}$	$3d_{3/2}$	$3d_{5/2}$
Γ_{nl}	14.70	25.04	2.71	5.31	0.07	0.09
nl	$4p_{1/2}$	$4p_{3/2}$	$4d_{3/2}$	$4d_{5/2}$	$5p_{1/2}$	$5p_{3/2}$
Γ_{nl}	0.62	1.25	0.02	0.02	0.10	0.20

The sumation over m_1 and m_2 in Eq. (19) is given in Appendix B and leads to the result of the partial PFBIC coefficient in this channel

$$R_{PFBIC}^{KXM_1} = \sum_{j_3, j_p} S(j_3, j_p) \frac{\alpha_d \Gamma_{KXM_1}(j_3, j_p)}{2\pi[\Delta^2 + (\Gamma_h + \Gamma_{3s}/2)^2]}, \quad (20)$$

where $S(j_3, j_p)$, $\Gamma_{KXM_1}(j_3, j_p)$ are, respectively, a statistical factor and the partial K-shell Auger width for PFBIC.

Using Eqs. (14), (16), and (20) we can define a total internal conversion coefficient R_{PFBIC} by

$$R_{PFBIC} = R_{PFBIC}^{\gamma_1 \gamma_2} + R_{PFBIC}^{\gamma_1, LM_1} + R_{PFBIC}^{KXM_1}. \quad (21)$$

III. NUMERICAL RESULTS FOR BIC DECAY OF ^{197}Au IN DIFFERENT CHARGE STATES

We now consider the numerical evaluation of PFBIC decay in ^{197}Au. The low-lying nuclear levels of ^{197}Au are shown in Fig. 3, together with the electronic energy levels for the case of the neutral atom. The computation of the electronic matrix elements was performed with the use of the RAINE Dirac-Fock computer package designed for electronic structure calculations as well as for the calculation of internal conversion coefficients in atoms [28–30]. Quantum electrodynamic (QED) corrections to the energy levels, including vacuum polarization and the self-energy of the electrons were computed using the GRASP code [31]. The $1s \rightarrow 3s$ transition energy in the neutral atom obtained by this method is found to be 77 291 eV that compares with an experimental value of 77 300 eV [24]. This difference gives an estimate of the accuracy of the transition energies used in the following numerical calculations.

A. Neutral atom

The contributions to the radiative width of the $1s$ hole state in the neutral atom are shown in Table I. All results have been calculated using the length gauge. The total radiative width of the $1s$ state is found to be 50.13 eV. The $2p \rightarrow 1s$ width per $2p$ electron $\Gamma_{\gamma}^{2p \rightarrow 1s} \simeq \Gamma_{2p \rightarrow 1s}$ is estimated to be $39.74/6 \simeq 6.5$ eV. Taking into account a contribution of approximately 4% from Auger transitions [24], we adopt a value of $\Gamma_h \simeq 52$ eV, and the total width of $\Gamma_h^{(t)} \simeq 59$ eV. The QED correction is nearly constant for all the configurations, and amounts to an energy shift approximately equal to -145 eV. The energy $\epsilon_{3s} - \epsilon_{1s}$ of the electron transition $1s \rightarrow 3s$ is found to be 77 291 eV. The BIC coefficient for this transition, calculated at the energy of nuclear transition $\omega_n = 77\,351$ eV, is $\alpha_d(M1) = 60\,619$ eV. Partial Auger widths have been calculated by Chen *et al.* [32], $\Gamma_{LM_1Y}^{3s \rightarrow 2p_{1/2}} = 0.13$ eV and $\Gamma_{LM_1Y}^{3s \rightarrow 2p_{3/2}} = 0.22$ eV. These values are in close agreement with the values that can be deduced from the mean fluorescent yield in the L shell of Gold $\omega_{2p} = 0.32$, and the values for the radiative widths given in Table II. The calculated energies and the radiative widths for the transitions $3s \rightarrow 2p$ are listed in Table II. Substituting all the values in Eq. (14), we obtain a value for the coefficient $R_{PFBIC}^{\gamma_1 \gamma_2} = 0.026$. The value of the $R_{PFBIC}^{\gamma_1, LM_1}$ is directly obtained from Eq. (16) and the preceeding numerical value of $R_{PFBIC}^{\gamma_1 \gamma_2}$. In the neutral atom we have $R_{PFBIC}^{\gamma_1, LM_1} = 0.053$. The third contribution to PFBIC, corresponding to the one step Auger decay process, can be calculated from Eq. (20). Numerical values of Γ_{KXM1} have been obtained from the number of M_1 vacancies created in Gold per decay of one K-shell vacancy [24], which yield $R_{PFBIC}^{\gamma_1, LM_1} = 0.11$.

TABLE II. The energies ω and the radiative widths Γ_{γ} of the $3s \rightarrow 2p$ transitions in neutral atoms of Au.

	$3s \rightarrow 2p_{1/2}$	$3s \rightarrow 2p_{3/2}$
ω, eV	10343.4	8508.3
Γ_{γ}, eV	0.046	0.072

In the neutral atom we thus obtain a value of the total R_{PFBIC} coefficient, from Eq. (21), of $R_{PFBIC} = 0.19$. Table III summarizes the different contributions to PFBIC, together with the value of the BIC coeffient $\alpha_d(M1)$. The effect of this value of RPFBIC on the nuclear lifetime of the first excited state in ^{197}Au will be discussed in the next section.

For completeness, we have calculated the contributions of higher electron states to BIC transitions in the neutral atom. The contributions to RPFBIC are less than 10^{-5}. For $n > 6$, the ns orbital is vacant in the initial state with the result that the BIC transition is no longer Pauli-forbidden and the value of contribution of bound internal conversion is then given by Eq. (15). In this case the R_{BIC} has a maximum value for $n = 6$, of $R_{BIC} = 2.210^{-4}$, which is again significantly smaller than the value of R_{PFBIC} given above.

B. Effect of ionization on the PFBIC process

In order to examine the magnitude of the charge state dependence of PFBIC, we have computed the bound internal conversion coefficient in ions up to 69^+. The results are shown in Table III. For each value of the charge state, we give in Table III the electronic configuration, the calculated energy mismatch, and the contributions to PFBIC from the three processes considered above. In these calculations we have assumed that the values of $\Gamma_{2p \rightarrow 1s}$, Γ_h, and Γ_h^t and ω_{2p} are independent of charge state since the effect of electron screening on the inner shells is very weak. Futhermore, up to charge state 61^+ we assume that the partial Auger widths remains constant.

TABLE III. Calculated values of the energy of the resonance defect Δ, the discrete conversion coefficient α_d^{M1}, and the PFBIC conversion coefficient R for various ions of ^{197}Au. Columns 5, 6, and 7 give, respectively, the contribution to R_{PFBIC} of the two photon process, $(R_{PFBIC}^{\gamma_1\gamma_2})$, the one photon and one electron process, $(R_{PFBIC}^{\gamma_1 LM_1})$, and the one step *K*-shell Auger process, $(R_{PFBIC}^{KXM_1})$. The last column gives the total PFBIC conversion coefficient, R_{PFBIC}. All of the values are in eV except the *R* coefficients that are dimensionless. For ions up to Au^{61+} the *R* value has been calculated from Eq. (21), whereas for the ions Au^{68+} and Au^{69+} the *R* value has been calculated from Eq. (15).

Ion	Configuration	Δ	α_d^{M1}	$R_{PFBIC}^{\gamma_1\gamma_2}$	$R_{PFBIC}^{\gamma_1 LM_1}$	$R_{PFBIC}^{KXM_1}$	R_{PFBIC}
Au^0	$[Xe]4f^{14}5d^{10}6s$	−60	606 19	0.026	0.053	0.11	0.19
Au^{11+}	$[Xe]4f^{14}$	−58	606 58	0.028	0.056	0.118	0.20
Au^{25+}	[Xe]	−102	610 29	0.010	0.020	0.043	0.074
Au^{33+}	$[Kr]4d^{10}$	−65	611 84	0.023	0.046	0.098	0.168
Au^{42+}	$[Kr]4d^1$	13	622 64	0.136	0.272	0.578	0.99
Au^{51+}	$[Ar]3d^{10}$	178	631 58	0.004	0.015	0.026	0.03
Au^{61+}	[Ar]	722	698 53	0.000	0.000	0.001	0.00
Au^{68+}	[Ne]3*s*	1258	753 74	0.000	0.000	0.000	0.39
Au^{69+}	[Ne]	1306	760 42	0.000	0.000	0.000	0.74

The principal factor contributing to the charge state dependence of the rate for the PFBIC process arises from the energy mismatch, Δ. As the atom is ionized from the neutral atom ($\Delta = -60$ eV), the PFBIC transition first moves away from resonance ($\Delta < 0$) until charge state 25^+ is attained and then moves back towards resonance. In ions with $q \simeq 41^+$ the Δ value lies only a few eV from exact resonance. As the charge state is further increased the Δ value becomes more positive and the transition moves rapidly away from resonance. These changes in the proximity to resonance are reflected in the values of R_{PFBIC} shown in the last column of Table III that attain a maximum value of 1.2 in the ion 40^+. Keeping in mind the uncertainty in the numerical values of the atomic transition energies (of the order of 10 eV) an accurate value of the charge state giving the maximum value of PFBIC is not possible. Nevertheless, it can be asserted than R_{PFBIC} reaches a maximum value of the order of unity around charge state $q = 40 \pm 2$.

When the charge state 69^+ is reached the ions have just ten electrons and the 3*s* shell is vacant so that excitation to the 3s shell can occur without violation of the Pauli principle. In this case the *R* value shown in Table III has been calculated from Eq. (15). The value of Δ is 1306 eV, which is ~19 times larger than that for the neutral atom. Despite this difference in the energy mismatch, the bound internal conversion coefficient in Au^{69+} turns out to have a value of 0.74, which is significantly larger than that for the neutral atom.

In the case of the ion Au^{68+}, only one of the 3*s* orbitals is occupied in the initial state. It is, therefore, possible for BIC decay to occur with excitation to the unoccupied 3*s* orbital without violating the Pauli principle. The probability for this process is approximately a half of that for BIC decay in the 69-fold ions, giving a value of $R = 0.39$ for Au^{69+}.

IV. DISCUSSION

In order to consider the effect of PFBIC on the nuclear decay we recall that the radiative nuclear transition has mixed multipolarity $M1+E2$, with the mixing parameter $\delta = -0.368 \pm 0.014$ [24]. We have performed calculations of the internal conversion coefficient (ICC) in the neutral atom and in different ionic states, namely, the 10^+ ion, which was experimentally studied in Ref. [33], and the 40^+ ion, where the PFBIC attains maximum of its value. Table IV shows values of the total internal conversion coefficients for the $M1$ and $E2$ transitions, calculated for the nuclear transition energy $\omega_n = 77\,351$ eV. Using these values along with the above mixing parameter δ, we find the total ICC in the neutral atom has a value, $\langle\alpha\rangle = 4.24$, in accordance with a literature value. We also note that the dependence of $\langle\alpha\rangle$ on the charge state is very weak.

The PFBIC process constitutes a new channel for the decay of the first excited state in Au. Taking into account this channel leads to an effective internal conversion coefficient

$$\alpha = \langle\alpha\rangle + R_{PFBIC}. \tag{22}$$

In the neutral atom the effect of R_{PFBIC} on α is small. Taking PFBIC into account changes the value of α by only 5%, a change that lies within the uncertainty in the experimental determination of α. Several points are of interest in connection with the different contributions to PFBIC. First, in spite of the small value of the gold *K*-shell fluorescence yield, less than 4%, the *K*-Auger BIC process is the dominant contribution to PFBIC. Eq. (20), which gives the intensity in this channel, is formally identical to Eq. (15), reflecting the fact

TABLE IV. The total conversion coefficients $\beta(M1)$ and $\alpha(E2)$ for the $M1$ and $E2$ transitions, and their average value $\langle\alpha\rangle$ for the 77 351 eV transition in ^{197}Au, with the mixing parameter $\delta = -0.368$, for various degrees of ionization of the electron shell.

Atom	$\beta_{tot}(M1)$	$\alpha_{tot}(E2)$	$\langle\alpha\rangle$
Au	2.745	15.26	4.238
Au^{10+}	2.747	15.29	4.243
Au^{42+}	2.758	15.45	4.272

that in this case the conversion is a one step process. Second, it is interesting to compare the rate for PFBIC and BIC for hypothetical transitions with the same value of the energy mismatch Δ. Since, as we show in the numerical calculations discussed below, $\Gamma_{3s\to 2p} \ll \Gamma_h$ and $\Gamma_h^{(t)} \approx \Gamma_h$, the ratio of the rates for PFBIC and BIC from Eqs. (14) and (15), apart from the geometrical factor S, is given approximately by

$$\frac{R_{PFBIC}}{R_{BIC}} \approx \left(\frac{\Gamma_\gamma^{3s\to 2p}}{\Gamma_h}\right)\left(\frac{\Gamma_\gamma^{2p\to 1s}}{\Gamma_h}\right). \tag{23}$$

Thus, in the case of identical Δ values, BIC decay via an intermediate state that violates the Pauli principle necessarily has a decay rate less than that for BIC decay via a Pauli-allowed intermediate state. The factor by which the rate for PFBIC decay is less than that for BIC decay is approximately equal to the product of the two ratios of widths on the right hand side of Eq. (23). Each of these width ratios represents the width of an $E1$ radiative transition divided by the total width of the 1s hole. In other words, the probability for PFBIC relative to BIC turns out to be proportional to the product of the lifetimes, $T \sim \hbar/\Gamma$, of each Pauli-forbidden intermediate state. In the limit $T \to \infty$ of a real stable state, the PFBIC process becomes strictly forbidden, as expected. It is noteworthy that this is not the case for BIC decay, which is not forbidden by the exclusion principle.

The half-life of this nuclear transition has been extensively studied. A mean value of 1.91 ns is reported for the half-life of the 77 351 eV nuclear state in the data tables of Ref. [24]. In the neutral atom, the inclusion of PFBIC changes the nuclear lifetime by only about 3.6%. In this case the influence of BIC on the nuclear lifetime thus turns out to be small. The situation is rather different in Au ions. As seen in Table III the value of R_{PFBIC} reaches a maximum, $R_{PFBIC} \simeq 1$ around charge state $q \simeq 40$. In this case, the inclusion of PFBIC would increase the value α by an amount of the order of 20%. A change of the value of α induces a change in the half-life $T_{1/2}$ of the nuclear level. The value $T_{1/2}^q$ is related to the value $T_{1/2}^0$ in the neutral atom by the relation [25]

$$T_{1/2}^q = T_{1/2}^0 \frac{1+\langle\alpha\rangle}{1+\langle\alpha\rangle+R_{PFBIC}}. \tag{24}$$

In ions of ^{197}Au with $q \simeq 40+$ the half-life is then shortened to $T_{1/2}^{40} \simeq 1.6$ ns compared to $T_{1/2}^0 = 1.9$ ns in the neutral atom.

Attempts have already been made to measure the change of the conversion rate of the 77 351 eV level due to ionization of the atomic shell [33]. Half-live values of 1.91 ± 0.02 ns and 1.96 ± 0.08 ns have been obtained for the neutral atom and $\sim 10+$ ion, respectively. Therefore, no effect of the charge state was found within the error bars. The above calculations of the PFBIC contribution are consistent with these experimental results.

V. CONCLUSION

We have presented theoretical results for a new mode of internal conversion which takes place by excitation of an electron to a bound orbital that is occupied in the initial state. This process, which appears to violate the Pauli exclusion principle, can take place by virtue of the finite widths of the electron transitions that depopulate the Pauli-forbidden state.

Numerical calculations described above for ^{197}Au show that in the neutral atom the Pauli-forbidden internal conversion to bound states corresponds to a decay rate that is 19% of that for radiative nuclear decay. Since the conversion coefficient in the neutral atom has a value of approximately 4.2, this means that the PFBIC process contributes approximately 4% of the total internal conversion decay rate.

The resonant nature of Pauli-forbidden internal conversion has been found to lead to a significant charge-state dependence of the half-life in highly charged ions of ^{197}Au. Thus the half-life is predicted to decrease by approximately 15% from Au^{33+} to Au^{42+} and then to increase by 15% from Au^{42+} to Au^{51+}. Measurement of the half-life of such highly charged ions at the level of approximately 5% would thus allow experimental demonstration of this mode of internal conversion.

ACKNOWLEDGMENTS

This work was supported by a Grant from the Russian Fund for Basic Research No. 99-02-17550, by DTRA (USA) contract No. DTRA 01-99-M-0514, and by the NATO Program of the Portuguese Ministry of Science and Technology.

APPENDIX A

We start from the expression of the numerator in Eq. (12). We define $M^{\gamma 1 \gamma 2}$ to be the product of amplitudes for nuclear conversion F_c, for emisson of a photon with energy ω' from the $3s$ orbital to the intermediate state $F_\gamma(\omega'; 3s \to 2p_j)$, and for emission of a photon from the intermediate orbital to the $1s$ $F_\gamma(\omega''; 2p_j \to 1s)$,

$$M^{\gamma 1 \gamma 2} = F_c F_\gamma(\omega'; 3s \to 2p_j) F_\gamma(\omega''; 2p_j \to 1s). \tag{A1}$$

In terms of the reduced matrix elements H_c, $H_\gamma(\omega')$, $H_\gamma(\omega'')$, $M^{\gamma 1 \gamma 2}$ is given by

$$M^{\gamma 1 \gamma 2} = \sum_{m_1, m_2, \rho, \alpha} \frac{C(I_2 M_2 \lambda \rho | M_1 I_1) C(j_1 m_1 \lambda \rho | j_2 m_2) C(j \alpha 1 \zeta | j_2 m_2) C(j_1 m_1 1 \eta | j \alpha)}{(2I_1+1)^{1/2}(2j_2+1)(2j+1)^{1/2}} H_c H_\gamma(\omega') H_\gamma(\omega''), \tag{A2}$$

where I_1, I_2 are the nuclear spins in the initial and final states, M_1 and M_2 are the associated magnetic quantum numbers, λ is the multipolarity of the nuclear transition, ρ is the associated magnetic quantum number, j_1 and j_2 are the total angular momenta of the converted electron in the initial $1s$ and final $3s$ orbitals, with m_1 and m_2 the associated magnetic quantum numbers, ζ and η are the magnetic quantum numbers of the two emitted photons, whilst j and α are the angular momentum quantum numbers of the electron in the intermediate state. The quantities $C(jmLM|j'm')$ are Clebsch-Gordan coefficients.

After summation over the magnetic quantum numbers m_1, m_2, leading to the same intermediate state spin projection $\alpha=m_1+\zeta$, $\alpha=m_2-\eta$, and using explicit values for the nuclear spins $j_1=1/2$, $j_2=1/2$, we obtain for the nuclear transition in ^{197}Au,

$$M^{\gamma_1\gamma_2}=\frac{1}{\sqrt{6}}\sum_{\rho} C(I_2M_2\lambda\rho|M_1I_1)W(1/2,1,1/2,1;j\lambda) \times C(1\,\eta 1\,\zeta|\lambda\rho)H_c^{\lambda}H_{\gamma}(\omega')H_{\gamma}(\omega''), \tag{A3}$$

where W is a $6j$ symbol. Inserting Eq. (A3) in Eq. (12) we have

$$F_{PFBIC}=\frac{M^{\gamma_1\gamma_2}}{\left(\Delta+i\frac{\Gamma_{3s\to 2p}+\Gamma_h}{2}\right)\left(\omega_n-\omega'-\epsilon_{2p}+i\frac{\Gamma_{2p\to 1s}+\Gamma_h}{2}\right)}. \tag{A4}$$

The expression for the decay width passing through a particular intermediate state, j, is then

$$\Gamma^{j}_{PFBIC}=\frac{2\pi}{(2I_1+1)}\sum_{\rho}\int |F_{PFBIC}|^2 d\omega', \tag{A5}$$

where the summation extands over magnetic quantum numbers leading to the intermediate state j.

We call Γ_c^{λ} the partial width for a discrete conversion between bound states for a multipolarity λ, [27]. The partial width for BIC is

$$\Gamma_c^{\lambda}=\frac{2\pi}{(2I_1+1)}\sum_{m_1,m_2,M_1,M_2,\rho} C^2(I_2M_2\lambda\rho|I_1M_1) \times C^2(j_1m_1\lambda\rho|j_2m_2)|H_c^{\lambda}|^2. \tag{A6}$$

The partial atomic radiative widths per vacancy have the following forms:

$$\Gamma^{\gamma}_{3s\to 2p}=\frac{2\pi}{(2j+1)^2}\sum_{\alpha\zeta} C^2(j\alpha 1\zeta|j_2m_2)|H_{3s\to 2p}|^2, \tag{A7}$$

$$\Gamma^{\gamma}_{2p\to 1s}=\frac{2\pi}{(2j_1+1)^2}\sum_{m_1\eta} C^2(j_1m_1 1\,\eta|j\alpha)|H_{2p\to 1s}|^2. \tag{A8}$$

Using the particular values of the nuclear and atomic spins involved in the transition in ^{197}Au, and inserting the definitions of the partial widths given in Eqs. (A6), (A7), and (A8), we obtain, after integration over the photon energy, ω', the following expression for $\Gamma^{\gamma_1\gamma_2}_{PFBIC}$:

$$\Gamma^{\gamma_1\gamma_2}_{PFBIC}=\Gamma_c\sum_j |W(1/2,1,1/2,1;j1)|^2\frac{(2j+1)}{\pi\Gamma_h^t} \times\frac{\Gamma^{\gamma}_{3s\to 2p}\Gamma^{\gamma}_{2p\to 1s}}{\Delta^2+\left(\frac{\Gamma_{3s\to 2p}+\Gamma_h^{(t)}}{2}\right)^2}, \tag{A9}$$

where $\Gamma_h^{(t)}$ is the combined width of the $1s$ hole and the width of the $2p\to 1s$ radiative transition.

Finally, the width Γ_c can be expressed in terms of the discrete conversion coefficient between the $1s$ and $3s$ orbitals, α_d, and the partial radiative width of the nuclear transition [27],

$$\Gamma_c=\alpha_d\Gamma_{\gamma}^{n}. \tag{A10}$$

This leads to the final expression for $\Gamma^{\gamma_1\gamma_2}_{PFBIC}$ given in Eq. (13).

APPENDIX B

We start from the expression in the numerator of Eq. (19). We define M^{KXM_1} to be the product of amplitudes F_c for nuclear conversion, and F^{KXM_1}, for K-shell Auger transitions.

$$M^{KXM_1}=\sum_{m_1,m_2,m}\frac{C(I_2M_2\lambda\rho|M_1I_1)C(j_1m_1\lambda\rho|j_2m_2)C(j_2m_2lm|j_pm_p)C(j_1m_1lm|j_3m_3)}{(2I_1+1)^{1/2}(2j_2+1)^{1/2}(2j_p+1)^{1/2}(2j_3+1)^{1/2}}H_cH_{au}, \tag{B1}$$

where H_c and H_{au} are the reduced matrix elements for internal conversion and K-shell Auger transitions respectively. In Eq. (B1) j_p and m_p stand for the spin and magnetic quantum number of the electron in the continuum state, whilst l and m refer to the angular momentum quantum numbers of the virtual photon. The summation over magnetic quantum numbers in Eq. (B1) runs over values leading to the same final electronic states j_3, j_p. Carrying out these summations yields

$$M^{KXM_1}=\frac{1}{\sqrt{2(2j_p+1)}}C(I_2M_2\lambda\rho|M_1I_1)W(j_3,j_1,j_p,j_2;l1)C(j_3m_3\lambda\rho|j_pm_p)H_cH_{au}. \tag{B2}$$

The width of the process, $\Gamma_{PFBIC}^{KXM_1}$, can be expressed in terms of the nuclear partial width for conversion, Γ_c, Eq. (A10), and the partial width per *K*-shell vacancy for *K*-shell Auger decay Γ_{KXM_1},

$$\Gamma_{PFBIC}^{KXM_1}=\Gamma_c\sum_{j_3 j_p}\frac{W(j_3,j_1,j_p,j_2;l1)^2|H_{au}|^2}{\Delta^2+\left(\frac{\Gamma_h+\Gamma_{3s}}{2}\right)^2}, \tag{B3}$$

where H_{au} is related to Γ_{KXM_1} by

$$\Gamma_{KXM_1}(j_1,j_2,j_3)=\frac{2\pi}{2j_1+1}\sum_{m_1,m_2,m,j_p,m_p}|H_{au}|^2. \tag{B4}$$

Summing over the quantum numbers yields

$$\Gamma_{KXM_1}(j_1,j_2,j_3)=\frac{2\pi}{(2j_1+1)(2l+1)}|H_{au}|^2. \tag{B5}$$

Dividing both sides of Eq. (B3) by Γ_n and using Eq. (B5) one finally obtains Eq. (20) for the width of the process.

[1] R.P. Feynman, Phys. Rev. **76**, 749 (1949).
[2] J. Goldstone, Proc. Roy. Soc. **239**, 267 (1957).
[3] R.J. Glauber and P.C. Martin, Phys. Rev. **95**, 572 (1954); *ibid.* **104**, 158 (1956); *ibid.* **109**, 1307 (1958).
[4] I.S. Batkin, Yu.G. Smirnov, and T.A. Churakova, Yad. Fiz. **33**, 968 (1981) [Sov. J. Nucl. Phys. **33**, 510 (1981)].
[5] I.S. Batkin, Yad. Fiz. **29**, 903 (1979) [Sov. J. Nucl. Phys. **29**, 464 (1979)].
[6] I.S. Batkin and M.I. Berkman. Yad. Fiz. **32**, 972 (1980) [Sov. J. Nucl. Phys. **32**, 502 (1980)].
[7] J.N. Bahcall, Phys. Rev. **128**, 2683 (1963); **132**, 362 (1963); Nucl. Phys. **71**, 267 (1965).
[8] E. Vatai, Nucl. Phys. A **156**, 541 (1970).
[9] W. Bambinek, H. Behrens, M.H. Chen, B. Craseman, M.L. Fitzpatrick, K. Ledingham, H. Genz, M. Mutterer, and R.L. Intelmann, Rev. Mod. Phys. **49**, 77 (1977).
[10] M.R. Harston and N.C. Pyper, Phys. Rev. A **45**, 6282 (1992).
[11] D. Guo, Phys. Rev. A **36**, 4267 (1987).
[12] X. Mu and B. Craseman, Phys. Rev. Lett. **57**, 3039 (1986).
[13] L.P. Rapoport, B.A. Zon, and N.L. Monakov, *Theory of Many-Photon Processes in Atoms* (Atomizdat, Moscow, 1978) (In Russian).
[14] K. Ilakovac, J. Tudoric-Ghemo, B. Busic, and V. Horvat, Phys. Rev. Lett. **56**, 2469 (1986).
[15] L.C. Angrave, N.E. Booth, R.J. Gaitskell, G.L. Salmon, and M.R. Harston, Phys. Rev. Lett. **80**, 1610 (1998).
[16] F.F. Karpeshin *et al.*, Phys. Rev. C **55**, 1665 (1997).
[17] M.R. Harston, T. Carreyre, J.F. Chemin, F.F. Karpeshin, and M.B. Trzhaskovskaya, Nucl. Phys. A **676**, 143 (2000).
[18] T. Carreyre, M.R. Harston, M. Aiche, F. Bourgine, J.F. Chemin, G. Claverie, J.P. Goudour, J.N. Scheurer, F. Attalah, J. Kiener, A. Lefebre, J. Durrell, J.P. Grandin, W.E. Meyerhof, and W. Phillips, Phys. Rev. C **62**, 024311 (2000).
[19] M. Morita, Prog. Theor. Phys. **49**, 1574 (1973).
[20] F.F. Karpeshin, I.M. Band, and M.B. Trzhaskovskaya, Nucl. Phys. A **654**, 579 (1999).
[21] M.R. Harston and J.F. Chemin, Phys. Rev. C **59**, 2462 (1999).
[22] S. Kishimoto, Y. Yoda, M. Seto, Y. Kobayashi, S. Kitao, R. Haruki, T. Kawauchi, K. Fukutani, T. Okano, Phys. Rev. Lett. **85**, 1831 (2000).
[23] M. Harston, Nucl. Phys. A **690**, 447 (2001).
[24] R.B. Firestone, *Table of Isotopes*, 8th ed., edited by V.S. Shirley (Wiley, New York, 1996), Vol. II.
[25] F. Attallah, M. Aiche, J.F. Chemin, J.N. Scheurer, W.E. Meyerhof, J.P. Grandin, P. Aguer, G. Bogaert, C. Grunber, J. Kiener, A. Lefebvre, and J.P. Thibaud, Phys. Rev. Lett. **75**, 1715 (1995).
[26] A.I. Akhiezer and V.B. Berestetsky, *Quantum Electrodynamics* (Nauka, Moscow, 1969).
[27] F.F. Karpeshin, I.M. Band, M.B. Trzhaskovskaya, and M.A. Listengarten, Phys. Lett. B **372**, 1 (1996).
[28] I.M. Band and M.B. Trzhaskovskaya, ADNDT **55**, 43 (1993).
[29] I.M. Band, V.I. Fomichev, PNPI Report No. 498, Leningrad, 1979 (unpublished).
[30] I.M. Band, M.A. Listengarten, and M.B. Trzhaskovskaya, PNPI Report No. 1479, Leningrad, 1989 (unpublished).
[31] B.J. McKenzie, I.P. Grant, and P.H. Norrington, Comput. Phys. Commun. **21**, 233 (1980).
[32] M.H. Chen, B. Crasemann, and H. Mark, ADNDT **24**, 13 (1979).
[33] U. Ulrickson, R. Hensler, D. Gordon, N. Benczer-Koller, and H. De Waard, Phys. Rev. **9**, 326 (1974).